IEEE Access
Multidisciplinary | Rapid Review | Open Access Journal

Received November 6, 2017, accepted December 12, 2017, date of publication December 14, 2017,
date of current version February 14, 2018.

Digital Object Identifier 10.1109/ACCESS.2017.2783443

Robust Test Statistic for Cooperative Spectrum Sensing Based on the Gerschgorin Circle Theorem

DAYAN ADIONEL GUIMARÃES
National Institute of Telecommunications, Santa Rita do Sapucaí 37540-000, Brazil
(dayan@inatel.br)

This work was supported by Finep with Funttel resources through the Radiocommunications Reference Center Project of Inatel under Grant 01.14.0231.00.

ABSTRACT The Gerschgorin circle theorem was recently applied to build two detectors for the purpose of spectrum sensing in cognitive radio applications, the so-called Gerschgorin radius-based and the Gerschgorin disk-based detectors. However, the corresponding test statistics do not exhibit the constant false alarm rate (CFAR) property and are not robust against dynamical noise, the situation in which nonuniform noise levels fluctuate over time. In this paper, a novel and simple detector for cooperative or multi-antenna spectrum sensing is proposed. The test statistic is the ratio between the sum of the Gerschgorin radii and the sum of the Gerschgorin centers relative to the covariance matrix of the signal received from one or more transmitters. It is named Gerschgorin radii and centers ratio (GRCR) detector. The GRCR exhibits the CFAR property and is robust against nonuniform and dynamical noise and received signal powers, yet being able to detect time-uncorrelated or time-correlated transmitted signals over additive Gaussian noise and fading channels.

INDEX TERMS Cognitive radio, Gerschgorin circle theorem, robust spectrum sensing.

I. INTRODUCTION

The spectrum sensing [1] is a crucial task within the cognitive radio (CR) framework [2]. It enables the negotiated or opportunistic access of CR-enabled secondary user (SU) terminals to vacant bands in a network of primary user (PU) terminals, thus alleviating the problems of congestion and scarcity of the radio-frequency spectrum inherited by the current fixed allocation policy. The cooperative spectrum sensing (CSS) is prevailing among several approaches, due to its capability of mitigating channel fading, shadowing and the hidden node problems by taking advantage of spatial diversity [1]. In centralized CSS, the received signal samples collected by the SUs or the SUs' local decisions are sent to a fusion center (FC), where they are combined to allow for the global decision upon the occupation of the sensed band. Owing to the cooperation, more reliable global decisions are obtained when compared to local SUs' decisions.

Several detection schemes have been proposed so far for the purpose of spectrum sensing, for instance the energy detection, the matched filter detection, the cyclostationary feature detection and several eigenvalue-based detection schemes [1], [3]. Cyclostationary detection needs to know the cyclic frequencies of the PU signal, and matched filtering requires the knowledge of the PU waveforms and the channel from the PU to the SUs. On the other hand, energy detection and eigenvalue-based detection do not need any information on the channels between the primary transmitter and the SUs, neither on the signal to be detected.

The energy detector and some eigenvalue-based detectors are semi-blind, i.e. they rely on the knowledge of the noise power, thus being vulnerable to the inaccuracies of the noise variance estimates, which is usually referred to as noise uncertainty. Moreover, energy detection is optimal for detecting independent and identically distributed (i.i.d.) signals [4]. Its performance degrades when detecting time-correlated signals, which is the case for most practical applications, mainly due to filtering effects [3]. Some eigenvalue-based spectrum sensing schemes can cope with both i.i.d. and non-i.i.d. (n.i.i.d.) signals [3]. There are other techniques, including some eigenvalue-based ones, that are totally blind, meaning that they do not need to know the noise variance as well.

The most known eigenvalue-based detection techniques are those built from the generalized likelihood ratio test (GLRT), the maximum-minimum eigenvalue detection (MMED), also known as eigenvalue ratio detection (ERD), and the maximum eigenvalue detection (MED), also known as Roy's largest root test (RLRT) [5]. Among these, the RLRT is considered the best in several

circumstances, but likewise the energy detection it needs to know the noise power for decision, thus being prone to noise uncertainty. The RLRT is an asymptotically optimum nonparametric detector under the Neyman-Pearson criterion for the case of a single unknown signal immersed in Gaussian noise with known variance [5]. In the generalized energy detection (GED) [6], which is an improved variation of the conventional energy detection, the problem of high sensitivity to noise uncertainty remains [7].

A spectrum sensing technique that is robust against noise uncertainty is not necessarily insensitive to nonuniform noise, a situation in which the noise variances are different among the SUs' receivers. Moreover, a spectrum sensing technique that is robust against nonuniform noise is not necessarily insensitive to nonuniform and dynamical noise, when the noise levels vary over time.

Nonuniform noise arises, for instance, due to uncalibrated receivers, different noise powers affecting the receivers, receivers subjected to different temperatures, and intentional or unintentional interference. The dynamics is observed when at least one of these phenomena vary over time. In the case of sensing techniques that need to know the noise variances, the nonuniform and dynamical noise condition may also arise from the fluctuations of the noise estimates as well.

Hence, the development of spectrum sensing strategies that are robust against nonuniform and dynamical noise is not simply a desirable design guideline. Due to the high chance of encountering those impairments in practice, it is in fact mandatory that the spectrum sensing technique is immune to them. This paper proposes such a technique.

A. RELATED WORK

A GLRT-based spectrum sensing method is proposed in [8] to operate with receivers subjected to different and unknown variances and arbitrary signal-to-noise ratios (SNRs). The resultant test is called Hadamard ratio (HR) test.

The performance of the Hadamard ratio test is analytically investigated in [9]. Specifically, the authors have derived approximate, but very accurate closed-form expressions for computing the probability of detection of the HR test.

A variant of the Hadamard ratio test, named noncircular Hadamard ratio (NC-HDM) test, is devised in [10] to cope with the important case of noncircular (NC) or improper primary signals [10], [11]. The key idea of [10] is to explore the complementary covariance matrix [12] of the received signal, besides the ordinary covariance matrix, to achieve improved performances and robustness in the n.i.i.d. noise scenario. Examples of digital modulation schemes that produce improper complex baseband signals are binary phase-shift keying (BPSK), pulse amplitude modulation (PAM), Gaussian minimum-shift keying (GMSK), offset quaternary phase-shift keying (OQPSK), and baseband (but not passband) orthogonal frequency-division multiplexing (OFDM) [12, p. 27]. Even proper baseband signals may become improper at the receiver due to imbalance between their in-phase and quadrature (I/Q) components, which is the case, for example, of quaternary phase-shift keying (QPSK) signals [12, p. 28].

The GLRT approach is applied in [13] to the situation in which there is no information on the number of PU signals. The resultant detector was called arithmetic to geometric mean (AGM) detector.

Two detectors for spectrum sensing are proposed in [14], both exploring the volume associated to the received signal sample covariance matrix (SCM), to distinguish between the presence or absence of the PU signal. The resulting volume-based detectors (VD) were named VD1 and VD2. The former is blind, whereas the latter needs the knowledge of the noise variance estimate to form the test statistic. In spite of being blind, the VD1 outperforms the VD2 in most of the cases analyzed in [14], in terms of performance and robustness against nonuniform noise.

The analytical performance of the volume-based detector VD1 proposed in [14] is assessed in [15]. Specifically, expressions for computing the false alarm and the detection probabilities for the scenario of i.i.d. noise are derived, as well as for the theoretical computation of the decision threshold. Although based on approximations, those expressions are capable of providing quite accurate results.

In [16], two blind spectrum sensing methods whose test statistics are based on the Gerschgorin circle theorem were proposed. The Gerschgorin circle theorem is also applied to the wide-band spectrum sensing problem in [17]–[19], but it is not used to directly form the test statistics. Instead, a source number estimation technique based on the Gerschgorin theorem is applied to determine the number of active channels, and the decision rule is based on a predefined fraction of this number with largest sampling powers. Hence, the noise variance is not needed to make the decision on the channel occupation state. In fact, there are several proposals that consider the Gerschgorin disk estimator (GDE) or its variations to tackle the fundamental signal processing problem of estimating the number of sources; see for instance [20], [21] and references therein.

The problem of multiple antenna spectrum sensing is addressed in [22], taking into account the correlation between the received signals at different uncalibrated receivers in the presence of additive white Gaussian noise (AWGN). The test statistic combines the weighted estimates of the correlations between all antenna pairs. The performance of the proposed detector is optimized by tuning the weights. The special case of the test statistic proposed in [22] for two antennas can be interpreted as the Hadamard ratio test.

An important observation about the previous spectrum sensing techniques is that their performances were assessed under nonuniform but fixed (non-dynamical) noise variances. Unfair judgments about the performance gaps and about the performance ranking when multiple techniques are compared may arise from this nonuniform and fixed variance approach, as will be discussed later on in this paper.

The circular folding cooperative power spectral density split cancellation (CFCPSC) is one of the most recent blind and robust spectrum sensing methods proposed in the literature [23]. The test statistic is formed as a ratio between power spectral densities in which the noise variance terms present in the numerator and denominator are canceled-out. The CFCPSC is robust against nonuniform and dynamical noise, but demands signal power concentration in the sensed band, which limits its application range.

B. CONTRIBUTION AND ORGANIZATION OF THE ARTICLE

It seems that [16] is the single publication, so far, with a direct application of the Gerschgorin circle theorem to the construction of test statistics for spectrum sensing. However, the test statistics proposed in [16] do not exhibit the constant false alarm rate (CFAR) property. The CFAR is a crucial property of any detector for spectrum sensing or radar applications, since it enables the configuration of the decision threshold for a given target probability of false alarm, independently of the noise variance. In the methods proposed in [16], the noise variance information is eventually needed to set the decision threshold for a given target performance, which diminishes their practical appeal. Moreover, the methods derived in [16] are not robust against dynamical noise, as demonstrated later on in this paper.

Motivated by the above facts, a novel and simple technique for cooperative or multi-antenna spectrum sensing is proposed herein. The corresponding test statistic is formed by the ratio between the sum of the Gerschgorin radii and the sum of the Gerschgorin centers with respect to the covariance matrix of the signal received from a single PU transmitter or from multiple PU transmitters. The proposed test statistic is named Gerschgorin radii and centers ratio (GRCR). Extensive simulation results are presented and discussed to demonstrate the following main attributes of the GRCR:

- It is robust against dynamical noise and against dynamical received signal powers.
- It exhibits the constant false alarm rate property.
- It is among the simplest test statistics, since the most complex operation is the computation of the received signal sample covariance matrix.
- It outperforms most of the common blind detectors under nonuniform and dynamical noise variances, especially when large noise variance differences are considered.
- It works with single or multiple primary transmitters.
- It works in both AWGN and fading channels.
- It is capable of detecting time-correlated and time-uncorrelated PU signals.

As a byproduct, this paper can also be cast as a review of some of the most recent and powerful cooperative spectrum sensing techniques.

The remainder of the article is organized as follows: In Section II, the system model for the cooperative spectrum sensing problem is described. Section III is devoted to the proposed GRCR test statistic. Several competing detectors are presented in Section IV, along with a complexity analysis. Numerical results and discussions are given in Section V. Section VI concludes the paper and gives some directions for further contributions regarding the GRCR.

II. SYSTEM MODEL

Let a discrete-time multiple-input, multiple-output (MIMO) model in which m SUs collect mn samples (n samples per SU) of the received signal from s PU transmitters during the sensing interval. In the centralized CSS with data fusion, the samples from all SUs are sent to the FC to form the received signal matrix $\mathbf{Y} \in \mathbb{C}^{m\times n}$ given by

$$\mathbf{Y} = \mathbf{H}\mathbf{X} + \mathbf{V}, \tag{1}$$

where $\mathbf{H} \in \mathbb{C}^{m\times s}$ is the channel matrix with elements h_{ij}, $i = 1, 2, \ldots, m$, $j = 1, 2, \ldots, s$, representing the complex channel gains between the j-th PU and the i-th SU. These gains are assumed to be constant during the sensing interval, and independent and identically distributed (i.i.d.) between consecutive sensing rounds.

In order to consider the realistic situation of possibly different received signal powers across the SUs, for instance due to different channel attenuations between the PU transmitters and the SU receivers, the channel matrix $\mathbf{H}$ is given by

$$\mathbf{H} = \mathbf{G}\mathbf{A}, \tag{2}$$

where $\mathbf{A} \in \mathbb{C}^{m\times s}$ is the matrix whose elements are $\alpha_{ij} = 1$ for pure AWGN channels between the PU transmitters and the SU receivers, or α_{ij} are zero-mean complex Gaussian random variables having unitary second moment to represent flat and slow Rayleigh fading channels. The matrix $\mathbf{G} \in \mathbb{R}^{m\times m}$ in (2) is a diagonal gain matrix given by

$$\mathbf{G} = \operatorname{diag}\left(\sqrt{\frac{\mathbf{p}}{p_{\text{avg}}}}\right), \tag{3}$$

where $\mathbf{p} = [p_1, p_2, \ldots, p_m]^{\mathrm{T}}$ is the vector with the received signal powers in each SU, and $p_{\text{avg}} = \frac{1}{m}\sum_{i=1}^{m} p_i$ is the average received signal power over all SUs.

Without loss of generality, the overall channel power gain is unitary, meaning that each PU transmits with a constant power given by p_{avg}/s.

The matrix $\mathbf{X} \in \mathbb{C}^{s\times n}$ in (1) carries the samples of each PU signal on each of its rows. Two cases are considered here for the elements of $\mathbf{X}$: i) they are zero-mean i.i.d. complex Gaussian random variables, i.e. the PU signals are white noise; ii) they are drawn from a zero-mean baseband QPSK signal with τ samples per symbol, where τ controls the temporal correlation between samples ($\tau = 1$ for i.i.d. samples; $\tau = n$ for n.i.i.d. samples having maximum correlation).

In the case of uniform noise, $\mathbf{V} \in \mathbb{C}^{m\times n}$ is the matrix containing i.i.d. Gaussian noise samples with zero mean and variance σ^2, i.e $\mathbf{V} \sim \mathcal{NC}(0, \sigma^2\mathbf{I})$, with $\mathbf{I}$ being the identity matrix of order m. In the case of nonuniform noise, the elements of the i-th row of $\mathbf{V}$ have variance σ_i^2, $i = 1, \ldots, m$.

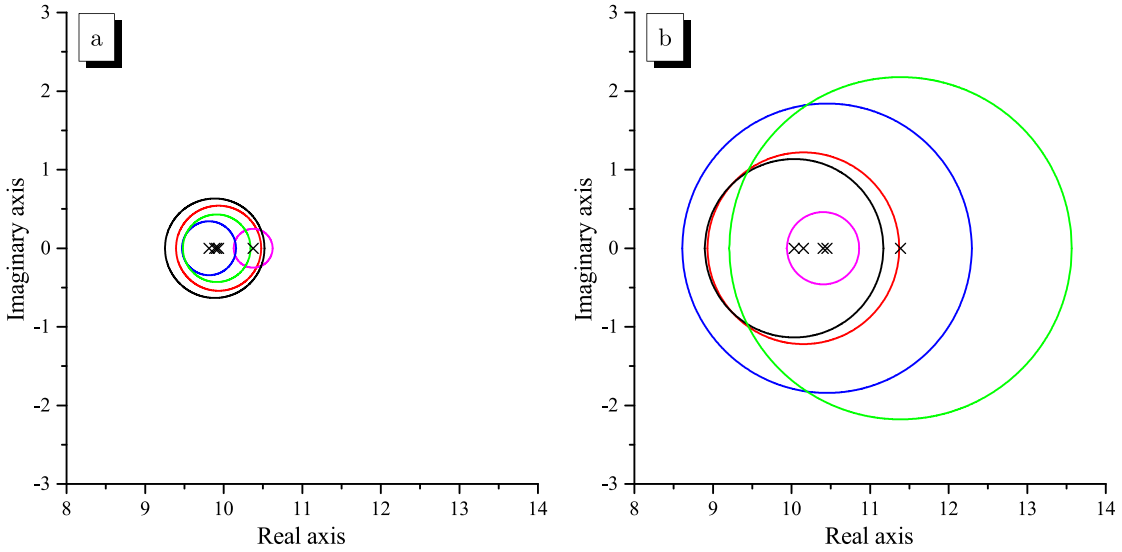

FIGURE 1. Gerschgorin disks under $\mathcal{H}_0$ (a) and $\mathcal{H}_1$ (b), for a sample covariance matrix **R** obtained from $m = 5$, $n = 5000$ and SNR $= -10$ dB. The marks x are the centers of the disks.

Denoting the average noise variance as $\sigma^2_{\text{avg}} = \frac{1}{m}\sum_{i=1}^{m}\sigma_i^2$, the received SNR, in dB, averaged over all SUs is given by

$$\text{SNR} = 10\log_{10}\left(\frac{p_{\text{avg}}}{\sigma^2_{\text{avg}}}\right). \tag{4}$$

The metrics typically used to assess the spectrum sensing performance are the probability of detection and the probability of false alarm, respectively defined as $P_{\text{d}} = \Pr(\text{decision} = \mathcal{H}_1|\mathcal{H}_1)$ and $P_{\text{fa}} = \Pr(\text{decision} = \mathcal{H}_1|\mathcal{H}_0)$, where $\mathcal{H}_1$ and $\mathcal{H}_0$ are the hypotheses of the presence (i.e. $\mathbf{Y} = \mathbf{HX} + \mathbf{V}$) and absence (i.e. $\mathbf{Y} = \mathbf{V}$) of the PU signals, respectively, and $\Pr(\cdot)$ is the probability of the underlying event.

A high value of P_{d} is desired to reduce the interference caused by the secondary network to the primary network due to missed detections. On the other hand, a low value of P_{fa} is aimed at, so that more opportunistic transmissions can be made by the secondary network due to bands that are less frequently declared occupied when they are actually vacant.

A typical tool for analyzing the above metrics simultaneously is the receiver operating characteristic (ROC) curve, which trades P_{fa} versus P_{d} by varying the decision threshold.

III. PROPOSED TEST STATISTIC

The sample covariance matrix of the received signal is computed by the FC as

$$\mathbf{R} = \frac{1}{n}\mathbf{Y}\mathbf{Y}^{\dagger}, \tag{5}$$

where $\dagger$ denotes the Hermitian operation (complex conjugate and transpose).

The Gerschgorin circle theorem [24, p. 82] states that the eigenvalues λ of **R** are located in the union of the m disks

$$|\lambda - r_{ii}| \leq \sum_{j\neq i}|r_{ij}|, \tag{6}$$

where r_{ij} is the element in the i-th row and j-th column of **R**, for $i, j = 1, \ldots, m$. The quantity $C_i = r_{ii}$ is the i-th center and the quantity $R_i = \sum_{j\neq i}|r_{ij}|$ is the corresponding radius of the Gerschgorin disk denoted as $D(C_i, R_i)$. In other words, the Gerschgorin circle theorem identifies a region in the complex plane containing the eigenvalues of a complex square matrix. Since every covariance matrix is positive semi-definite, then $C_i \in \mathbb{R}_+$, meaning that the Gerschgorin centers are located in the non-negative part of the real axis.

It has been found empirically that the ratio between the sum of the Gerschgorin radii and the sum of the Gerschgorin centers with respect to **R** has different behaviors under $\mathcal{H}_0$ and $\mathcal{H}_1$, being capable of serving as a test statistic for spectrum sensing. Based on this finding, the proposed Gerschgorin radii and centers ratio (GRCR) test statistic is defined as

$$T_{\text{GRCR}} = \frac{\sum_{i=1}^{m} R_i}{\sum_{i=1}^{m} C_i}. \tag{7}$$

The simple reasoning behind the construction of this test can be explained with the help of Fig. 1, where the Gerschgorin disks under $\mathcal{H}_0$ (a) and $\mathcal{H}_1$ (b) are shown for a sample covariance matrix **R** obtained from $m = 5$ SUs, $n = 5000$ samples per SU and SNR $= -10$ dB. Under $\mathcal{H}_0$, the eigenvalues of **R** are $[\lambda_1, \lambda_2, \lambda_3, \lambda_4, \lambda_5] \approx [10.44, 10.30, 9.90, 9.76, 9.51]$, the Gerschgorin radii are $[R_1, R_2, R_3, R_4, R_5] \approx [0.54, 0.25, 0.34, 0.63, 0.43]$, the Gerschgorin centers are $[C_1, C_2, C_3, C_4, C_5] \approx [9.93, 10.37, 9.81, 9.89, 9.91]$, $\sum R_i \approx 2.19$, $\sum C_i \approx 49.92$, and $T_{\text{GRCR}} \approx 0.04$. Under $\mathcal{H}_1$, the eigenvalues are $[\lambda_1, \lambda_2, \lambda_3, \lambda_4, \lambda_5] \approx [12.38, 10.43, 10.19, 9.82, 9.61]$, the Gerschgorin radii are $[R_1, R_2, R_3, R_4, R_5] \approx [1.22, 0.46, 1.84, 1.13, 2.18]$, the Gerschgorin centers are $[C_1, C_2, C_3, C_4, C_5] \approx [10.15, 10.40, 10.45, 10.03, 11.39]$, $\sum R_i \approx 6.83$, $\sum C_i \approx 52.42$, and $T_{\text{GRCR}} \approx 0.13$.

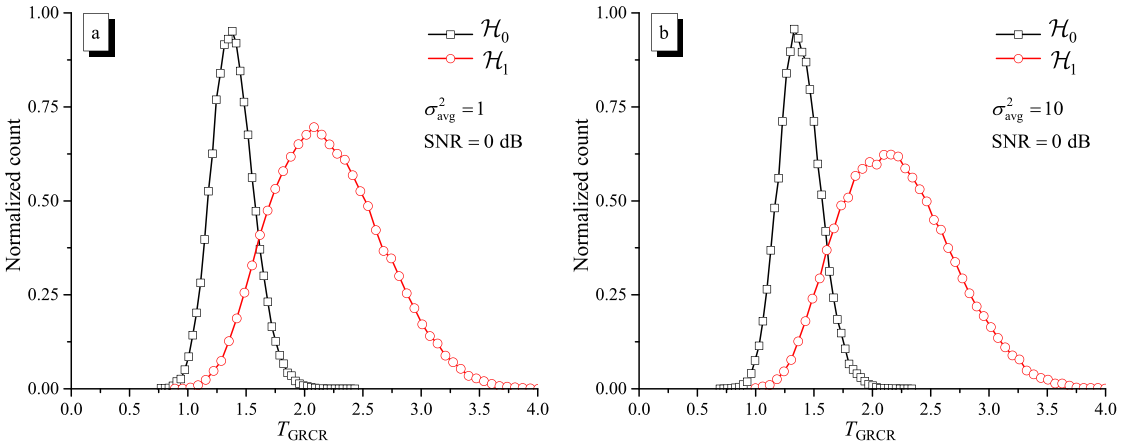

FIGURE 2. Histograms of the GRCR test (7) for $\sigma^2 = \sigma^2_{avg} = 1$ (a) and $\sigma^2 = \sigma^2_{avg} = 10$ (b), obtained from $m = 6$, $n = 10$ and SNR = 0 dB.

From this simple example, which corresponds to a low SNR condition, it can be noticed that the numerator of (7) has changed significantly from $\mathcal{H}_0$ to $\mathcal{H}_1$ (from 2.19 to 6.83), while the denominator has not changed significantly (from 49.92 to 52.42), producing an increase of about 3 times in T_{GRCR}. This means that T_{GRCR} under $\mathcal{H}_1$ departs from T_{GRCR} under $\mathcal{H}_0$ as the SNR increases, which is a necessary condition for the test statistic to work properly. As expected, the discrimination between $\mathcal{H}_0$ and $\mathcal{H}_1$ becomes poorer in lower SNR regimes, which also happens with other detectors. The numerical results in Section V confirm these statements.

Detection would be possible by the sole computation of $\sum R_i$, but it is the division by $\sum C_i$ that brings the CFAR property to the test statistic (7).

Figure 2 shows the histograms obtained from 50000 values of the test statistic (7) for each of the hypotheses, under uniform noise with $\sigma^2 = \sigma^2_{avg} = 1$ (a) and $\sigma^2 = \sigma^2_{avg} = 10$ (b), $m = 6$ SUs, $n = 10$ samples per SU, and SNR $= 0$ dB. In this illustration the transmitted powers were adjusted to keep the SNR fixed for both values of σ^2_{avg}, according to (4). It can be seen that the histograms under $\mathcal{H}_0$ are identical in shape and support, meaning that the proposed test statistic has the CFAR property. In other words, if the decision threshold is set to yield the desired false alarm rate for a given noise variance at the input of the SUs' receivers, this false alarm rate will not change if the noise variance is changed.

The Algorithm 1 synthesizes the steps of the proposed GRCR cooperative spectrum sensing technique.

Algorithm 1 Steps of the GRCR Spectrum Sensing

1) Each of the m SUs in cooperation collects n samples of the received signal during the sensing interval and transmits them to the FC.
2) The FC forms the matrix $\mathbf{Y} \in \mathbb{C}^{m\times n}$ defined in (1) with the received samples, and computes the covariance matrix $\mathbf{R} \in \mathbb{C}^{m\times m}$ using (5).
3) The FC computes $C_i = r_{ii}$ and $R_i = \sum_{j\neq i} |r_{ij}|$, where r_{ij} is the element in the i-th row and j-th column of $\mathbf{R}$, and forms the GRCR test statistic T_{GRCR} using (7).
4) The FC decides in favor of the presence of the PU signal if $T_{GRCR} > \xi$ and decides in favor of the absence of the PU signal otherwise, where ξ is the decision threshold configured to achieve the desired CFAR.

IV. COMPETING TEST STATISTICS

In this section, the test statistics used for comparisons with the proposed one are described in a concise way, aiming at giving to the present paper a self-contained character. Some of them are robust against nonuniform noise, a few are robust against nonuniform and dynamical noise, and others are not robust at all. All test statistics discussed in this section exhibit the CFAR property, except the Gerschgorin radius-based and the Gerschgorin disk-based tests described in Section IV-C.

The choice of the competing test statistics described in the sequel was made based on their popularity and newness, also taking into account implementation complexities that are not very away from each other, aiming at fairness in the subsequent comparisons.

Among the techniques reported in Section I-A, the NC-HDM of [9] was not considered due to the fact of being derived for noncircular received signals, which is not the scenario targeted by the majority of the detectors proposed in the literature so far. The VD2 test of [14] was not chosen because of having worse performance than the VD1. The detectors that do not use the Gerschgorin theorem to form the test statistic were not considered either, which is the case of the ones proposed in [17]–[19]. The multi-antenna spectrum sensing technique proposed in [22] was not chosen due to the relatively high complexity of finding the weights used in the test statistic. Finally, the reason for not considering the CFCPSC of [23] was twofold: i) its exhibits a high algorithmic complexity, in spite of the relatively simple operations performed in each step; ii) it demands that the PU signal

spectrum has some power concentration, i.e. it has to occupy a fraction of the sensed band.

A. ENERGY DETECTOR TEST STATISTICS

The most simple and known semi-blind detector is the energy detector (ED), whose test statistic is

$$T_{\mathrm{ED}} = \frac{1}{\sigma^2} \sum_{i=1}^{m} \sum_{j=1}^{n} |y_{ij}|^2, \tag{8}$$

where y_{ij} is the element in the i-th row and j-th column of the received signal matrix $\mathbf{Y}$. In the nonuniform noise scenario, the ED becomes

$$T_{\mathrm{EDnu}} = \sum_{i=1}^{m} \frac{1}{\sigma_i^2} \sum_{j=1}^{n} |y_{ij}|^2. \tag{9}$$

The statistical power of the test (8) is inferior to the test (9), since the latter makes full use of the knowledge of the noise variances in all SUs' receivers.

B. EIGENVALUE-BASED TEST STATISTICS

In eigenvalue-based CSS, spectral holes are detected using test statistics built from the eigenvalues of the sample covariance matrix defined in (5). Representing the ordered eigenvalues of $\mathbf{R}$ as $\lambda_1 \geq \lambda_2 \geq \cdots \geq \lambda_m$, the test statistics for the classical GLRT for a single PU signal and uniform noise, the MMED (or ERD) and the MED (or RLRT) are computed at the FC according to [5]

$$T_{\mathrm{GLRT}} = \frac{\lambda_1}{\sum_{i=1}^{m} \lambda_i}, \tag{10}$$

$$T_{\mathrm{MMED}} = \frac{\lambda_1}{\lambda_m}, \tag{11}$$

$$T_{\mathrm{MED}} = \frac{\lambda_1}{\sigma^2}. \tag{12}$$

In the nonuniform noise scenario, the MED becomes

$$T_{\mathrm{MEDnu}} = \frac{\lambda_1}{\sigma_{\mathrm{avg}}^2}. \tag{13}$$

Since there is no way of using the different noise variances in the case of the MED, the test (13) has a reduced statistical power when subjected to nonuniform noise.

If there is no information on the number of PU signals, the GLRT approach yields the so-called arithmetic to geometric mean (AGM) detector [13], whose test statistic is

$$T_{\mathrm{AGM}} = \frac{\frac{1}{m} \sum_{i=1}^{m} \lambda_i}{\left(\prod_{i=1}^{m} \lambda_i \right)^{\frac{1}{m}}}. \tag{14}$$

The tests (10), (11) and (14) are blind, whereas the tests (12) and (13) are semi-blind. Semi-blind detectors need the noise variance information, being inherently prone to noise uncertainty, which is also the case of the energy detector.

C. GERSCHGORIN RADIUS-BASED AND GERSCHGORIN DISK-BASED TEST STATISTICS

Motivated by the fact that the Gerschgorin disks $D(C_i, R_i)$ are poor representations of the location of the eigenvalues of $\mathbf{R}$, in [16] a transformed covariance matrix $\mathbf{R}'$ is used instead of $\mathbf{R}$. The matrix $\mathbf{R}'$ is constructed from a unitary transformation on $\mathbf{R}$ that preserves its eigenvalues, but reduces the Gerschgorin radii, as follows. Firstly, matrix $\mathbf{R}$ is partitioned according to

$$\mathbf{R} = \begin{bmatrix} r_{11} & \cdots & r_{1m} \\ r_{21} & \cdots & r_{2m} \\ \vdots & \ddots & \vdots \\ r_{m1} & \cdots & r_{mm} \end{bmatrix} = \begin{bmatrix} \mathbf{R}_1 & \mathbf{r} \\ \mathbf{r}^\dagger & r_{mm} \end{bmatrix}, \tag{15}$$

where $\mathbf{R}_1$ is called the leading sub-matrix of $\mathbf{R}$, with order $(m-1) \times (m-1)$. This matrix is formed by removing the m-th row and the m-th column of $\mathbf{R}$. The vector $\mathbf{r}$ of length $m-1$ is formed by the m-th column of $\mathbf{R}$ without the element r_{mm}. The leading sub-matrix $\mathbf{R}_1$ is then factored as $\mathbf{R}_1 = \mathbf{U}\mathbf{D}\mathbf{U}^\dagger$, where $\mathbf{U}$ is a unitary matrix of order $(m-1) \times (m-1)$ formed by the eigenvectors of $\mathbf{R}_1$, and $\mathbf{D}$ is a diagonal matrix of the same order, whose main diagonal is formed by the eigenvalues of $\mathbf{R}_1$. From $\mathbf{U}$, the unitary transformation matrix $\mathbf{T}$ is constructed according to

$$\mathbf{T} = \begin{bmatrix} \mathbf{U} & \mathbf{0} \\ \mathbf{0}^{\mathrm{T}} & 1 \end{bmatrix}, \tag{16}$$

where $\mathbf{0}$ is the all-zero vector of length $m-1$. Finally, the transformed covariance matrix is given by

$$\mathbf{R}' = \mathbf{T}^\dagger \mathbf{R} \mathbf{T} = \begin{bmatrix} \mathbf{D} & \mathbf{U}^\dagger \mathbf{r} \\ \mathbf{r}^\dagger \mathbf{U} & r_{mm} \end{bmatrix}. \tag{17}$$

Writing the eigenvector matrix as $\mathbf{U} = [\mathbf{u}_1, \mathbf{u}_2, \ldots, \mathbf{u}_{m-1}]^{\mathrm{T}}$, where $\mathbf{u}_i$ is the eigenvector corresponding to the i-th largest eigenvalue, the Gerschgorin radius-based (GR) test statistic proposed in [16] is

$$T_{\mathrm{GR}} = |\mathbf{u}_1^\dagger \mathbf{r}|. \tag{18}$$

The Gerschgorin disk-based (GD) test statistic proposed in [16] is given by

$$T_{\mathrm{GD}} = \frac{\frac{1}{m-1} \sum_{i=1}^{m} d_{ii}}{\left(\prod_{i=1}^{m} d_{ii} \right)^{\frac{1}{m-1}}} |\mathbf{u}_1^\dagger \mathbf{r}|. \tag{19}$$

where d_{ii} is the element in the i-th row and column of $\mathbf{D}$.

It can be noticed that T_{GR} and T_{GD} need the eigen-decomposition of the leading sub-matrix $\mathbf{R}_1$, thus being more complex than the proposed T_{GRCR} in (7). However, the important observation concerning (18) and (19) is that these test statistics do not exhibit the CFAR property, although this attribute is claimed in [16].

To illustrate the non-CFAR property of the GR and the GD tests, Figs. 3 and 4 respectively show the histograms obtained from 50000 values of the test statistics (18) and (19) for each of the hypotheses, under uniform noise with $\sigma^2 =$

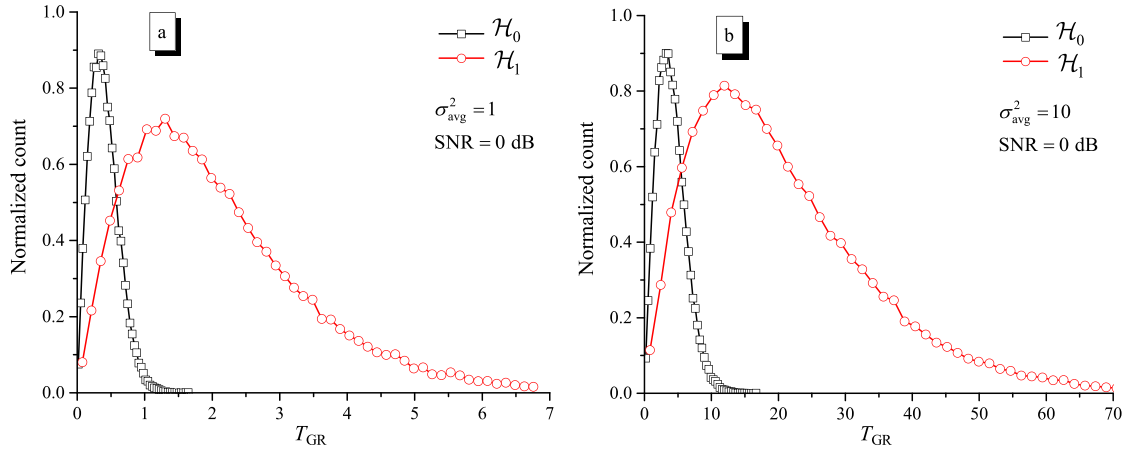

FIGURE 3. Histograms of the GR test (18) for $\sigma^2 = \sigma^2_{avg} = 1$ (a) and $\sigma^2 = \sigma^2_{avg} = 10$ (b), obtained from $m = 6$, $n = 10$ and SNR = 0 dB.

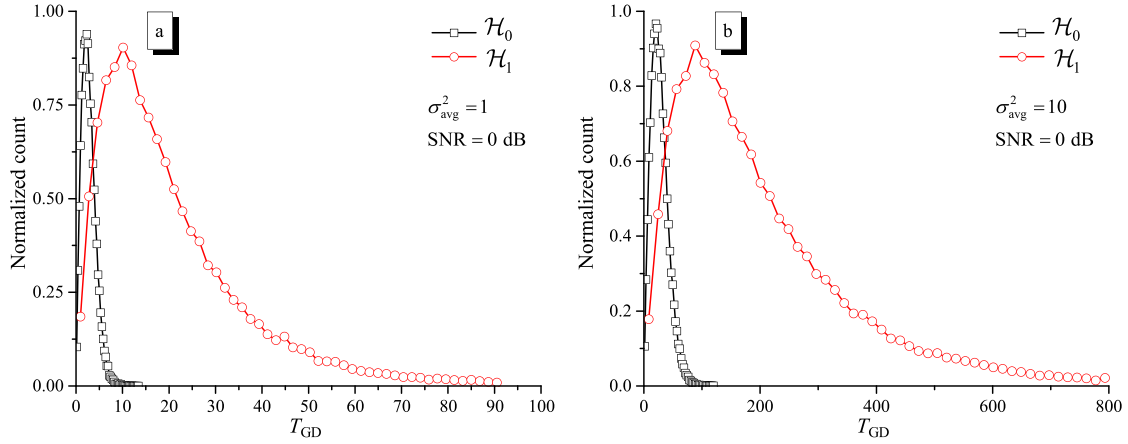

FIGURE 4. Histograms of the GD test (19) for $\sigma^2 = \sigma^2_{avg} = 1$ (a) and $\sigma^2 = \sigma^2_{avg} = 10$ (b), obtained from $m = 6$, $n = 10$ and SNR = 0 dB.

$\sigma^2_{\text{avg}} = 1$ (a) and $\sigma^2 = \sigma^2_{\text{avg}} = 10$ (b), $m = 6$ SUs, $n = 10$ samples per SU, and SNR $= 0$ dB. In these illustrations the power of the signal transmitted by the SU was adjusted to keep the SNR fixed for both values of σ^2_{avg}, according to (4). It can be seen that the ranges of variation of the decision threshold under $\mathcal{H}_0$, i.e. the support of the histograms, are not the same under different noise powers, meaning that the GR and the GD test statistics do not exhibit the CFAR property. In other words, if the decision threshold is set to yield the desired false alarm rate for a given noise variance at the input of the SUs' receivers, this false alarm rate will change if the noise variance changes. A detector that exhibits the CFAR property does not change its false alarm rate, no matter the noise variance is.

D. HADAMARD RATIO TEST STATISTIC

The GLRT-based spectrum sensing method proposed in [8] to operate with uncalibrated receivers yields the so-called Hadamard ratio (HR) test statistic

$$T_{\text{HR}} = \frac{\det(\mathbf{R})}{\prod_{i=1}^{m} r_{ii}}, \tag{20}$$

where $\det(\mathbf{R})$ is the determinant of $\mathbf{R}$.

The HR is one of the most powerful detectors in the presence of nonuniform noise, yet having a relatively low complexity [14].

E. VOLUME-BASED TEST STATISTIC

The volume-based detector 1 (VD1) proposed in [14] is shown to be robust against nonuniform noise variances, possibly outperforming the HR detector when the noise variances remain unchanged over the sensing rounds, i.e., in the nonuniform and non-dynamical noise condition. The VD1 test statistic is

$$T_{\text{VD1}} = \log\Big[\det(\mathbf{E}^{-1}\mathbf{R})\Big], \tag{21}$$

where $\mathbf{E}^{-1}$ is the inverse of the matrix $\mathbf{E} = \text{diag}(\mathbf{d})$, where $\text{diag}(\mathbf{d})$ forms a diagonal matrix whose main diagonal is composed of the elements of the vector $\mathbf{d} = [d_1, d_2, \cdots, d_m]$. The i-th element of $\mathbf{d}$ is the Euclidean norm of the i-th row of $\mathbf{R}$, that is, $d_i = \|\mathbf{R}(i, :)\|_2$.

It can be noticed that the complexity of the VD1 is higher than the HR, since the former involves the computation of the

logarithm of the determinant of a product of two matrices, one being the sample covariance matrix and the other being the inverse of a matrix derived from the sample covariance matrix.

In order to reach the final decision upon the occupancy of the sensed channel, the test statistic T selected among (7), (8), (9), (10), (11), (12), (13), (14), (18), (19), (20) and (21) is compared with the decision threshold ξ, which is computed to yield the target values of $P_{\rm d}$ and $P_{\rm fa}$. For the above detectors, $P_{\rm d} = \Pr(T > \xi|\mathcal{H}_1)$ and $P_{\rm fa} = \Pr(T > \xi|\mathcal{H}_0)$, except in the cases of the HR test (20) and the VD1 test (21), for which $P_{\rm d} = \Pr(T_{\rm HR} > \xi|\mathcal{H}_0)$ and $P_{\rm fa} = \Pr(T_{\rm HR} > \xi|\mathcal{H}_1)$ [8], [14].

F. COMPUTATIONAL COMPLEXITIES

The processing time required for computing the test statistic (7) for the proposed GRCR test is mostly owed to the computation of the sample covariance matrix $\mathbf{R}$, which costs $\mathcal{O}(nm^2)$ floating-point operations [25].

The energy detection test statistic (8) is the less complex. Its computational cost is dominated by the nm multiplications, thus yielding a complexity of $\mathcal{O}(nm)$.

The complexity of the eigenvalue-based test statistics (10), (11), (12) and (14) is determined by the complexity associated to the sample covariance matrix computation, i.e. $\mathcal{O}(nm^2)$, plus the complexity related to the eigenvalue computation, which costs $\mathcal{O}(m^3)$ [20].

The GR and GD tests (18) and (19), respectively, need to compute the sample covariance matrix $\mathbf{R}$ with complexity $\mathcal{O}(nm^2)$, plus the extra burden of $\mathcal{O}((m-1)^3)$ to perform the eigen-decomposition of the leading sub-matrix $\mathbf{R}_1$, resulting in complexity growths comparable to the eigenvalue-based test statistics.

For the HR test (20), the computation of the sample covariance matrix $\mathbf{R}$ costs $\mathcal{O}(nm^2)$, and the burden to calculate the determinant of $\mathbf{R}$ costs around $\mathcal{O}(m^3)$ or more.

In the case of the VD1 test statistic (21), the computational complexity is dominated by a cascade of the cost associated to the sample covariance matrix estimation, which is $\mathcal{O}(nm^2)$, and the cost of computing the determinant of a matrix of order m, which is $\mathcal{O}(m^3)$ or more. The inversion of $\mathbf{E}$ and posterior matrix multiplication $\mathbf{E}^{-1}\mathbf{R}$ are relatively simple operations, since $\mathbf{E}$ is a diagonal matrix.

In summary, the smallest computational complexity growth is achieved by the ED, followed by the GRCR and then by the other tests considered herein. Notice that the GRCR is m times more complex than the ED. As a consequence, in the typical scenario of cooperative spectrum sensing with a small number of SUs in cooperation, this represents a small complexity increase with respect to the ED. One must recall, however, that the ED is semi-blind and the GRCR is totally blind. Hence, to the best knowledge of the author, the proposed GRCR is the blind and robust test with lowest computational complexity growth.

V. NUMERICAL RESULTS AND DISCUSSIONS

Each point on the ROC curves shown hereafter was generated from 50000 Monte Carlo events simulating the generation of each test statistic under the hypotheses $\mathcal{H}_0$ and $\mathcal{H}_1$. The decision threshold ξ was varied from the minimum to the maximum values of each corresponding test statistic in 100 equally-spaced values. The values of $P_{\rm fa}$ versus $P_{\rm d}$ were determined from the empirical cumulative distribution function (CDF) computed from the counts of false alarm and detection events for each test statistic. Specifically, $P_{\rm fa} = 1 - c_T(t|\mathcal{H}_0)$ for $t = \xi$, and $P_{\rm d} = 1 - c_T(t|\mathcal{H}_1)$ for $t = \xi$, where $c_T(t|\mathcal{H}_0)$ and $c_T(t|\mathcal{H}_1)$ are the CDFs of the test statistic T under $\mathcal{H}_0$ and $\mathcal{H}_1$, respectively. Each value for the probability of detection on curves other than ROCs was computed from 10000 Monte Carlo events simulating the generation of each test statistic under the hypothesis $\mathcal{H}_1$. The channels between the PUs to the SUs were slow and flat Rayleigh fading channels.

A. PRELIMINARY RESULTS

Some preliminary results are provided in this subsection with the purpose of paving the way for the performance comparisons presented subsequently.

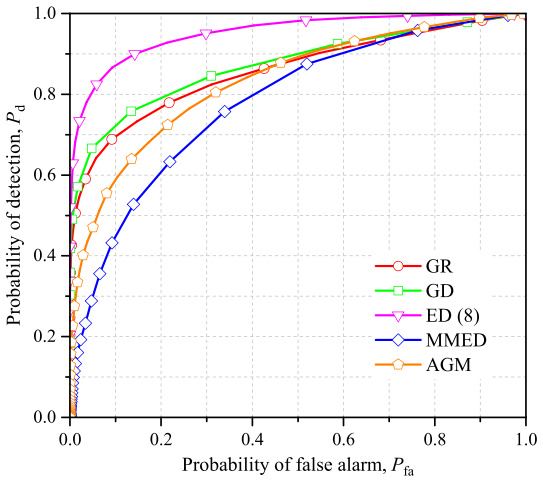

FIGURE 5. Performance of different detectors under uniform noise for $\sigma^2 = \sigma^2_{\rm avg} \approx 1.78$, $m = 6$, $n = 10$ and SNR $= -3$ dB. These results are in agreement with [16, Fig. 3(a)]. This figure is better viewed in color.

Figure 5 gives ROC curves for the global spectrum sensing performance achieved by the test statistics GR, GD, ED, MMED and AGM, under uniform noise. In this case the noise variance is the same across all SUs; its value was set to $\sigma^2 \approx 1.78$. The other system parameters were chosen as $m = 6$ SUs, $n = 10$ samples per SU, SNR $= -3$ dB, single i.i.d. Gaussian PU signal, and uniform received powers. These parameters are the same as those adopted in [16, Fig. 3(a)].

The results shown in Fig. 5 are in agreement with [16, Fig. 3(a)], serving to validate the simulations. These results are also meant to be references for comparisons with Fig. 6 in terms of the consequence of having uni-

form or nonuniform noise variances at the input of the SUs' receivers.

Figure 6 considers the same system parameters used in Fig. 5, but now for a nonuniform noise scenario with $[\sigma_1^2, \sigma_2^2, \sigma_3^2, \sigma_4^2, \sigma_5^2, \sigma_6^2] \approx [3.02, 0.32, 4.37, 0.23, 2.24, 0.54]$, yielding $\sigma_{\text{avg}}^2 \approx 1.78$ and $\text{var}(\sigma_{\text{avg}}^2) \approx 2.90$. This set of variances are the same as those adopted in [16, Fig. 3(b)]. Notice in this figure that there are two curves for the ED, one using (8) and the other using (9). With the exception of the curve obtained using (9), the others are in agreement with [16, Fig. 3(b)]. The ED adopted in [16] is the test (8), which uses the unfair value of $\sigma^2 = \sigma_{\text{avg}}^2 \approx 1.78$, thus yielding a worse performance than the ED (9), which makes full use of the knowledge of σ_i^2, $i = 1, \ldots, 6$.

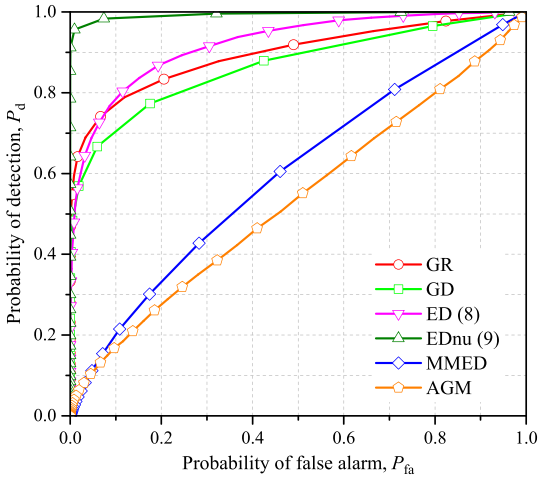

FIGURE 6. Performance of different detectors under nonuniform noise for $\sigma_{\text{avg}}^2 \approx 1.78$ and $\text{var}(\sigma_{\text{avg}}^2) \approx 2.90$, $m = 6$, $n = 10$ and SNR $= -3$ dB. Excluding the ED using (9), the remaining results are in agreement with [16, Fig. 3(b)]. This figure is better viewed in color.

The most relevant result of this subsection is presented in Fig. 7, complementing Figs. 5 and 6. The system parameters are the same as those in Fig. 6, but now it has been chosen a different set for the noise variances, that is $[\sigma_1^2, \sigma_2^2, \sigma_3^2, \sigma_4^2, \sigma_5^2, \sigma_6^2] \approx [0.81, 3.41, 0.12, 0.88, 1.08, 4.40]$, also yielding $\sigma_{\text{avg}}^2 \approx 1.78$ and $\text{var}(\sigma_{\text{avg}}^2) \approx 2.90$. It can be noticed that the detector performances have changed significantly compared to Fig. 6, with the exception of the ED due to the fact that noise variances are known. It can also be observed in Fig. 7 that the performances of the MMED and the AGM have exchanged their ranking with respect to Fig. 6.

From the results in Figs. 6 and 7, it can be concluded that the robustness of a given spectrum sensing technique under nonuniform noise, and even its performance relative to other techniques, cannot be fairly assessed by means of a single realization of the noise variances. The correct procedure is to vary the noise levels over the Monte Carlo events, which configures the nonuniform and dynamical noise scenario. This conclusion also extends to the case of unequal received signal powers, whose correct procedure is also to vary them over the sensing rounds.

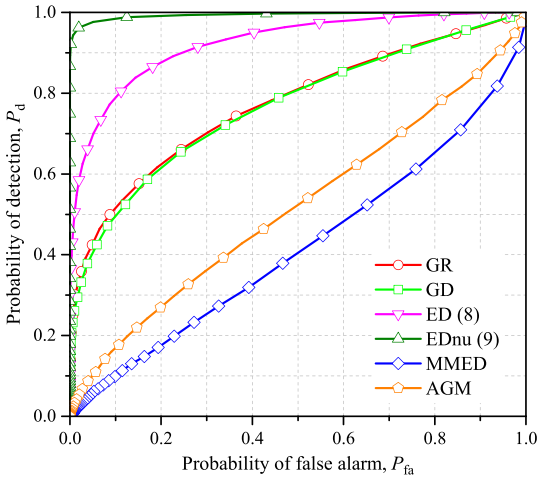

FIGURE 7. Performance of different detectors under another set of nonuniform noise with $\sigma_{\text{avg}}^2 \approx 1.78$ and $\text{var}(\sigma_{\text{avg}}^2) \approx 2.90$, $m = 6$, $n = 10$ and SNR $= -3$ dB. These results complement those in [16, Fig. 3]. This figure is better viewed in color.

Notice that the dynamical received powers and dynamical noise variances are consistent with a real spectrum sensing scenario in which signal and noise intensities are time-varying quantities due to time-varying receiver positions, temperatures, noise and interference sources. Hence, hereafter the nonuniform noise and nonuniform received signal power scenarios are simulated dynamically.

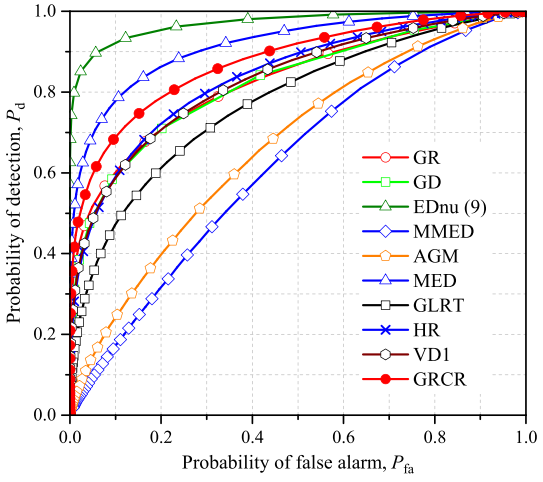

FIGURE 8. Performance of all detectors under nonuniform and dynamical noise $\sigma_i^2 \sim \mathcal{U}[0.05\sigma_{\text{avg}}^2, 1.95\sigma_{\text{avg}}^2]$, with $\sigma_{\text{avg}}^2 = 1.78$, for $m = 6$, $n = 10$ and SNR $= -3$ dB. This figure is better viewed in color.

B. PERFORMANCE OF THE PROPOSED AND THE COMPETING DETECTORS

Figure 8 shows ROC curves for all detectors considered in this paper under nonuniform noise, with noise variances drawn from a uniform distribution in each sensing round, that is $\sigma_i^2 \sim \mathcal{U}[0.05\sigma_{\text{avg}}^2, 1.95\sigma_{\text{avg}}^2]$, with $\sigma_{\text{avg}}^2 = 1.78$. As before, it has been adopted $m = 6$, $n = 10$, SNR $= -3$ dB, single i.i.d. Gaussian PU signal, and uniform received powers.

It can be seen from Fig. 8 that the GRCR is the blind detector with best performance, since it is only outperformed by the ED (9) and the MED, which are non-blind techniques that need the knowledge of the noise variances at the SUs' receivers. The detectors GR, GD, HR and VD1 have approximately the same performance in this scenario, but worse than the GRCR. The GLRT, the AGM and the MMED have poorer performances due to their high sensitivity to nonuniform noise.

An important aspect unveiled by Fig. 8 in favor of the GRCR technique is that it can achieve attractive performances using a relatively small number of samples (only 10 in the situation depicted in the figure). This is particularly interesting in applications requiring short sensing intervals, for instance to increase the throughput of the secondary network.

From this point on, only the spectrum sensing techniques that do not require the knowledge of the noise variance are evaluated. Thus the ED and the MED are excluded from the analyses. The GR and the GD are also excluded, since they do not exhibit the important property of CFAR. Among the eigenvalue-based techniques, only the classical GLRT is considered, since it is the best blind test statistic under unknown uniform noise and single PU signal [5], although it is not robust against nonuniform noise. The tests HR and VD1, which were designed for uncalibrated noise variances are also considered. In summary, the results shown hereunder are for the proposed GRCR (7), the GLRT (10), the HR (20) and the VD1 (21).

When nonuniform noise variances and nonuniform received powers are considered, their values in each sensing round were independently drawn from a uniform distribution, respectively as $\sigma_i^2 \sim \mathcal{U}[0.05\sigma_{\text{avg}}^2, 1.95\sigma_{\text{avg}}^2]$ and $p_i \sim \mathcal{U}[0.05p_{\text{avg}}, 1.95p_{\text{avg}}]$.

For the sake of conciseness, only QPSK primary signals are considered, since the detection of modulated signals is the most common situation in practice. It is attested, however, that i.i.d. Gaussian PU signals were also used under the same conditions, keeping the conclusions unchanged with respect to QPSK signals. The number of samples per QPSK symbol has been arbitrarily set to $\tau = 10$; see Section II.

An important performance measure of a spectrum sensing technique is the required SNR at which a given P_{d} is achieved for a fixed P_{fa}. For instance, the reference probabilities from the IEEE 802.22 standard for cognitive wireless regional area networks (WRANs) are $P_{\text{d}} \geq 0.9$ for a fixed $P_{\text{fa}} = 0.1$ [26], [27]. Hence, the CFAR has been fixed at 0.1 for all analyzed detectors. The required number of samples depends mainly on the specified sensing interval, on the detection technique and on the SNR. It has been fixed at $n = 500$, which is the value sufficient for the target P_{d} to be reached at low SNR values, as also required by the IEEE 802.22 standard.

Figure 9 shows the P_{d} versus the SNR for the analyzed detectors under uniform noise and received powers for $s = 1$ PU transmitter, $m = 6$ SUs and $n = 500$ samples collected by each SU. It can be seen that all detectors have comparable detection metrics, with a small advantage of the GLRT.

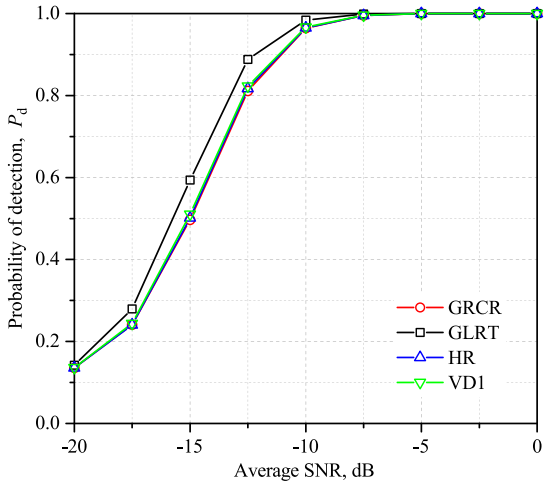

FIGURE 9. P_{d} versus SNR for $n = 500$, $s = 1$, $m = 6$, n.i.i.d. QPSK PU signal, uniform noise and received powers.

The above system parameters were also used to plot Fig. 10, now considering nonuniform noise variances and nonuniform received signal powers. It can be noticed that the classical GRLT is very sensitive to the dynamical variation of the noise and signal powers, whereas the other three detectors are robust. The detection capability of the HR has improved slightly from the uniform noise and signal powers to the nonuniform situation; the opposite has happened with the VD1. The GRCR has maintained exactly the same performance, which is attractive from the perspective of having a fixed performance for any noise or received signal variation about the corresponding averages.

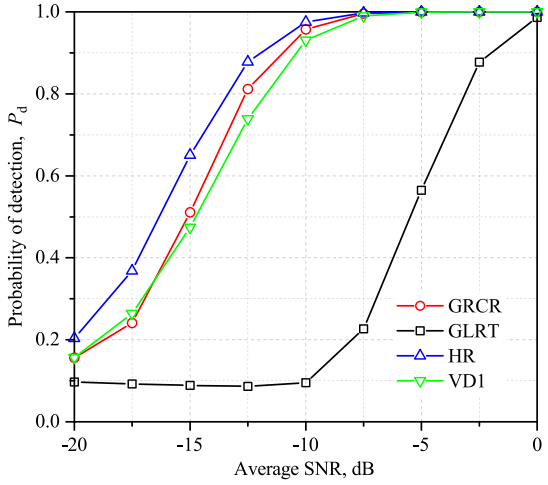

FIGURE 10. P_{d} versus SNR for $n = 500$, $s = 1$, $m = 6$, n.i.i.d. QPSK PU signal, nonuniform noise and received powers.

The number of PU transmitters is changed to $s = 3$ in Fig. 11, considering the uniform noise and received signal powers. The other system parameters are the same as those

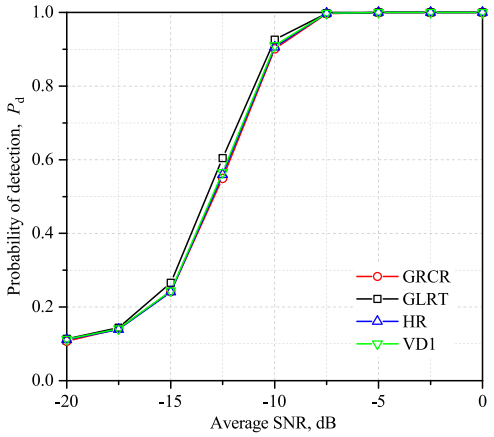

FIGURE 11. P_d versus SNR for $n = 500$, $s = 3$, $m = 6$, n.i.i.d. QPSK PU signals, uniform noise and received powers.

adopted in Fig. 9. The performances of all detectors are roughly the same, but reduced in comparison with the case of $s = 1$ (see Fig. 9). Such a reduction in the probability of detection with an increase in the number of transmitted signals has been also observed in [8].

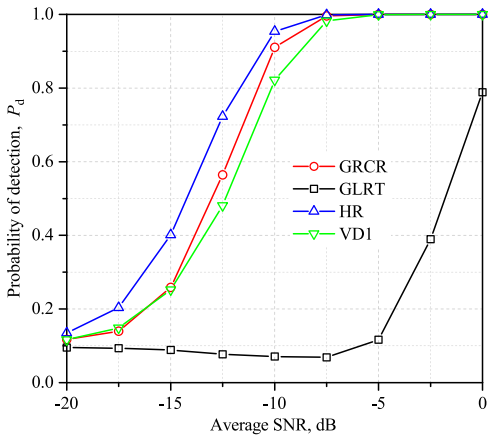

FIGURE 12. P_d versus SNR for $n = 500$, $s = 3$, $m = 6$, n.i.i.d. QPSK PU signals, nonuniform noise and received powers.

The number of PU transmitters is also $s = 3$ in Fig. 12, but now considering the scenario of nonuniform noise and nonuniform received signal powers. The other system parameters are the same as those adopted in Fig. 11. Again, the detection performance of the GLRT has been drastically affected with respect to the situation of uniform noise and signal powers shown in Fig. 11, while the other detectors remained robust, with a little improvement of the HR and a little penalty of the VD1. It can be noticed, one more time, that the performance of the proposed GRCR has not changed from the uniform to the nonuniform and dynamical noise and signal. When compared with Fig. 10, it can be observed in Fig. 12 that all detectors had their performances decreased with the increased number of PU transmitters.

VI. CONCLUSIONS

This paper has presented a novel and simple test statistic for cooperative or multi-antenna spectrum sensing. The test, which was named Gerschgorin radii and centers ratio (GRCR) test, is formed by the ratio between the sum of the Gerschgorin radii and the sum of the Gerschgorin centers relative to the covariance matrix of the signal received from a single or multiple transmitters.

The GRCR exhibits the CFAR property and is robust against nonuniform and dynamical noise and received signal powers, yet being capable of detecting time-uncorrelated or time-correlated transmitted signals over additive Gaussian noise and fading channels.

The performance of the GRCR is very close to the performances of leading robust detectors recently proposed in the literature, with the advantage of being simpler and keeping its performance metrics unchanged from the situation of uniform to nonuniform and dynamical noise and received signal powers. A clear advantage in performance over the analyzed robust detectors can be observed when a small number of samples is collected by the SUs. This is particularly attractive for short sensing time applications.

A complementary conclusion is related to the way in which the robustness of detectors under nonuniform noise and received signal powers must be assessed. The most common situation in practice is to have both noise and received powers varying over time, meaning that they must have dynamical behavior in models and simulations. The fixed noise and received signal powers setup must be avoided, unless it is intended to mimic a situation which is likely to happen in the real world.

A natural deployment of the proposed GRCR test statistic is to find its distribution under $\mathcal{H}_0$ and $\mathcal{H}_1$, so that, hopefully, closed-form expressions for calculating P_{fa}, P_{d} and the decision threshold ξ can be derived. This seems to be a formidable challenge that represents an opportunity for further contributions.

The computation of the GRCR test statistic could benefit from modern techniques for the efficient computation of the covariance matrix, like those described in [25]. The impact of using such techniques on the global spectrum sensing performance is also an interesting problem to be tackled.

REFERENCES

[1] I. F. Akyildiz, B. F. Lo, and R. Balakrishnan, "Cooperative spectrum sensing in cognitive radio networks: A survey," *Phys. Commun.*, vol. 4, no. 1, pp. 40–62, Mar. 2011.

[2] J. Mitola and G. Q. Maguire, Jr., "Cognitive radio: Making software radios more personal," *IEEE Pers. Commun.*, vol. 6, no. 4, pp. 13–18, Apr. 1999.

[3] Y. Zeng and Y.-C. Liang, "Eigenvalue-based spectrum sensing algorithms for cognitive radio," *IEEE Trans. Commun.*, vol. 57, no. 6, pp. 1784–1793, Jun. 2009.

[4] S. M. Kay, *Fundamentals of Statistical Signal Processing: Estimation Theory*. Upper Saddle River, NJ, USA: Prentice-Hall, 1993.

[5] B. Nadler, F. Penna, and R. Garello, "Performance of eigenvalue-based signal detectors with known and unknown noise level," in *Proc. IEEE Int. Conf. Commun.*, Jun. 2011, pp. 1–5.

[6] Y. Chen, "Improved energy detector for random signals in Gaussian noise," *IEEE Trans. Wireless Commun.*, vol. 9, no. 2, pp. 558–563, Feb. 2010.
[7] S. S. Kalamkar and A. Banerjee, "On the performance of generalized energy detector under noise uncertainty in cognitive radio," in *Proc. Nat. Conf. Commun. (NCC)*, Feb. 2013, pp. 1–5.
[8] D. Ramirez, G. Vazquez-Vilar, R. Lopez-Valcarce, J. Via, and I. Santamaria, "Detection of rank-*P* signals in cognitive radio networks with uncalibrated multiple antennas," *IEEE Trans. Signal Process.*, vol. 59, no. 8, pp. 3764–3774, Aug. 2011.
[9] L. Huang, Y. Xiao, H. C. So, and J. Fang, "Accurate performance analysis of Hadamard ratio test for robust spectrum sensing," *IEEE Trans. Wireless Commun.*, vol. 14, no. 2, pp. 750–758, Feb. 2015.
[10] L. Huang, Y. H. Xiao, and Q. T. Zhang, "Robust spectrum sensing for non-circular signal in multiantenna cognitive receivers," *IEEE Trans. Signal Process.*, vol. 63, no. 2, pp. 498–511, Jan. 2015.
[11] A. M. Sykulski and D. B. Percival, "Exact simulation of noncircular or improper complex-valued stationary Gaussian processes using circulant embedding," in *Proc. IEEE 26th Int. Workshop Mach. Learn. Signal Process. (MLSP)*, Sep. 2016, pp. 1–6.
[12] P. Schreier and L. Scharf, *Statistical Signal Processing of Complex-Valued Data the Theory of Improper and Noncircular Signals*. Cambridge, U.K.: Cambridge Univ. Press, 2010. [Online]. Available: https://books.google.com.br/books?id=HBaxLfDsAHoC
[13] R. Zhang, T. J. Lim, Y. C. Liang, and Y. Zeng, "Multi-antenna based spectrum sensing for cognitive radios: A GLRT approach," *IEEE Trans. Commun.*, vol. 58, no. 1, pp. 84–88, Jan. 2010.
[14] L. Huang, H. So, and C. Qian, "Volume-based method for spectrum sensing," *Digit. Signal Process.*, vol. 28, pp. 48–56, May 2014. [Online]. Available: https://doi.org/10.1016/j.dsp.2014.02.003
[15] L. Huang, C. Qian, Y. Xiao, and Q. T. Zhang, "Performance analysis of volume-based spectrum sensing for cognitive radio," *IEEE Trans. Wireless Commun.*, vol. 14, no. 1, pp. 317–330, Jan. 2015.
[16] R. Li, L. Huang, Y. Shi, and H. C. So, "Gerschgorin disk-based robust spectrum sensing for cognitive radio," in *Proc. IEEE Int. Conf. Acoust., Speech Signal Process. (ICASSP)*, May 2014, pp. 7278–7282.
[17] H. Qing, Y. Liu, and G. Xie, "Robust spectrum sensing for blind multiband detection in cognitive radio systems: A gerschgorin likelihood approach," *Trans. Internet Inf. Syst.*, vol. 7, no. 5, pp. 1131–1145, 2013. [Online]. Available: https://doi.org/10.3837/tiis.2013.05.011
[18] H. Qing, Y. Liu, G. Xie, K. Liu, and F. Liu, "Blind multiband spectrum sensing for cognitive radio systems with smart antennas," *IET Commun.*, vol. 8, no. 6, pp. 914–920, Apr. 2014.
[19] H. Qing, Y. Liu, G. Xie, and J. Gao, "Wideband spectrum sensing for cognitive radios: A multistage wiener filter perspective," *IEEE Signal Process. Lett.*, vol. 22, no. 3, pp. 332–335, Mar. 2015.
[20] L. Huang, T. Long, and S. Wu, "Source enumeration for high-resolution array processing using improved gerschgorin radii without eigendecomposition," *IEEE Trans. Signal Process.*, vol. 56, no. 12, pp. 5916–5925, Dec. 2008.
[21] Z. M. Liu, Z. Y. Lu, Z. T. Huang, and Y. Y. Zhou, "Improved gerschgorin disk estimator for source enumeration with robustness against spatially non-uniform noise," *IET Radar, Sonar Navigat.*, vol. 5, no. 9, pp. 952–957, Dec. 2011.
[22] Z. Pourgharehkhan, A. Taherpour, J. Sala-Alvarez, and T. Khattab, "Correlated multiple antennas spectrum sensing under calibration uncertainty," *IEEE Wireless Commun. Lett.*, vol. 14, no. 12, pp. 6777–6791, Dec. 2015.
[23] R. C. D. V. Bomfin, R. A. A. de Souza, and D. A. Guimarães, "Circular folding cooperative power spectral density split cancellation algorithm for spectrum sensing," *IEEE Commun. Lett.*, vol. 21, no. 2, pp. 250–253, Feb. 2017.
[24] J. W. Demmel, *Applied Numerical Linear Algebra*. Philadelphia, PA, USA: SIAM, 1997.
[25] X. Chen, M. R. Lyu, and I. King, "Toward efficient and accurate covariance matrix estimation on compressed data," in *Proc. 34th Int. Conf. Mach. Learn.*, Aug. 2017, pp. 767–776. [Online]. Available: http://proceedings.mlr.press/v70/chen17g.html
[26] C. C. Stevenson, G. Chouinard, Z. Lei, W. Hu, S. J. Shellhammer, and W. Caldwell, "IEEE 802.22: The first cognitive radio wireless regional area network standard," *IEEE Commun. Mag.*, vol. 47, no. 1, pp. 130–138, Jan. 2009.
[27] *IEEE 802 Part 22: Cognitive Wireless RAN Medium Access Control (MAC) and Physical Layer (PHY) Specifications: Policies and Procedures for Operation in the TV Bands*, IEEE Standard 802.22-2011, The Institute of Electrical and Electronic Engineers, 2011. [Online]. Available: http://standards.ieee.org/getieee802/download/802.22-2011.pdf

DAYAN ADIONEL GUIMARÃES received the Ph.D. degree in electrical engineering from the State University of Campinas, Unicamp, Brazil, in 2003. He is currently a Lecturer and a Researcher with the National Institute of Telecommunications, Inatel, Brazil. His research interests are the general aspects of fixed and mobile wireless communications, specifically radio propagation, digital transmission, spectrum sensing for cognitive radio, and convex optimization and signal processing applied to communications.